universitätbonn

E214 – ATLAS

Advanced Laboratory Course

Authors:
Groupe P9
Lina Zabawa – s6lizaba@uni-bonn.de
Nils Stausberg – s6nistau@uni-bonn.de

Tutors:
Elisabeth Schopf
Alessandra Betti

Date of Experiment:
22./23.03.2017

Contents

1 Introduction

In this experiment we want to get familiar with the physics at the Large Hadron Collider at CERN. The main focus thereby is on processes that are investigated by the ATLAS experiment and we are able to analyse real data of this detector.

2 Theoretically background

2.1 Particle physics

2.1.1 Standard model and fundamental particles

The aim of particle physics is to reduce all the observations back to one model with fundamental particles and forces. This model is called the standard model and shown in figure 1.

Today it is well established that the known matter has a substructure. The basic elements are structureless fundamental particles which are classified by their spin. Particles with half-integer spin are called fermions and particles with integer spin are called bosons. The fermions, more precisely leptons and quarks can be categorized in three families. Further so called gauge bosons exits, which are the exchange particles of the fundamental forces. The last piece of the model, the Higgs boson, is a scalar particle and was found a few years ago.

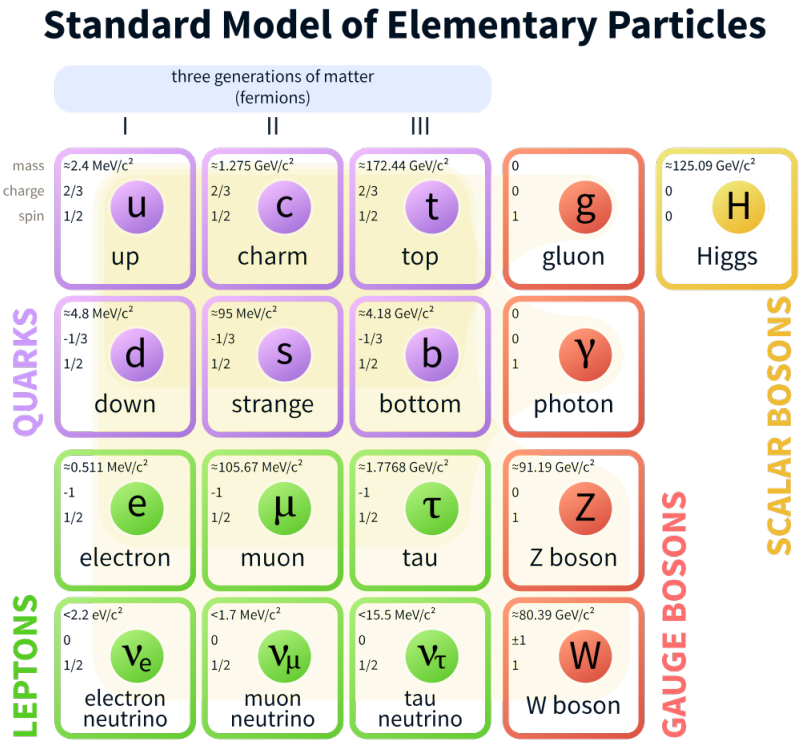

Figure 1: Standard Model of fundamental particles[Wik].

2.1.2 Fundamental forces

In nature four fundamental forces are known. The gravitational, the electromagnetic, the strong and the weak interaction. The gravitational force is understood as a continuous classical field[1], whereas

[1] A huge afford is going on also to discretize this interaction.

the other three, which are more important for particle physic, are modelled as discrete quantum fields.

The QED (quantum electrodynamics) describes the interaction between charged particles via electromagnetic interaction. The gauge boson is the massless photon. Dealing with this processes in analysis, we have to consider real and virtual radiation corrections. First one is caused by initial or final state radiation (real) and the latter one for example by vertex-corrections (virtual).

The gauge theory of the strong interaction is called QCD (quantum chromodynamics). In this theory the electric charge is being replaced by the colour charge and the photon as massless gauge boson by the gluon. The colour charge is an inner degree of freedom with three possible states (red, green and blue)[2]. One important difference to QED is the fact that in QCD not just quarks, but also gluons carry color. Due to this the running coupling constant depending on the momentum transfer or distance shows opposite behavior. At small distances or high momenta transfer we speak from asymptotic freedom, as for high distances or small momentum transfer the confinement effect can be found. Since gluons are carrying a color as well as a anti-color, nine different combination can be found. One of them is forbidden, so that in nature eight gluons are existing.

The last interaction is the weak interaction with $W^{\pm}$ and Z as gauge bosons. The W-boson for weak-charged currents and the Z-boson for weak-neutral currents. An important difference of this interaction to the other ones is that the gauge bosons carry mass, what is at first glance with respect to non-renormalisability not allowed. A solution for this problem can be found in the Higgs-mechanism and the spontaneous symmetry breaking which will be explained later on.

The weak and the electromagnetic interaction can be sumerized in the so called electroweak interaction. Here the photon and the Z^0 bosons are a mixing state of a triplet (W^1, W^2, W^3) and a singlet (Y). The mixing angle is called Weinberg or electroweak mixing angle.

2.1.3 Hadrons

Hadrons are bounded states of quarks (q) and/or anti-quarks ($\bar{q}$), whereas we distinguish between mesons (which are $q\bar{q}$ states) and baryons (which are three-quark-states). Due to the confinement effect, quarks can be just find as bounded states[3], where the overall color has to be white. Therefore the colour state of a meson is given through $\frac{1}{\sqrt{3}}(q_B\bar{q}_{\bar{B}} + q_G\bar{q}_{\bar{G}} + q_R\bar{q}_{\bar{R}})$ and of a baryon through $\frac{1}{\sqrt{6}}\epsilon_{ijk}q_iq_jq_k$.

2.1.4 The heavy gauge bosons

The Large-Hadron-collider (LHC) is a proton-proton-accelerator with a ring based structure at CERN. The most important process for the generation of the heavy gauge bosons W and Z is the weak Drell-Yan-process, although besides this there are also $2 \to 2$-processes with W-boson emission. During the lab course we observe the decays of the bosons into stable leptons, because electrons and muons are quite easy to determine concerning the signature they leave in the detector.

The $W^{\pm}$ and Z^0 bosons are produced with a small transverse momentum, compared to the mass of the bosons. Looking at the production-process to lowest order we even expect a transverse momentum of zero because of the collinearity of the partons. Unconsidered by this is a non zero probability to generate other partons. This would produce a recoil and with that a transverse momentum unequal to zero.

[2]For anti particle anti-red, anti-green and anti-blue holds.

[3]An exception is the t-quark, which has such a short lifetime that it decays nearly immediately.

2.2 The standard model and beyond

2.2.1 Higgs mechanism

In the standard model the Higgs field is postulated as an $SU(2)_L$-doublet complex scalar field, that means with a spin of zero.

$$\Phi = \begin{pmatrix} \Phi_1 \\ \Phi_2 \end{pmatrix}$$

This field exhibits four degrees of freedom, from which three are giving mass to W^+, W^- and Z^0. The last degree of freedom can be observed as a free particle, the Higgs-boson.

2.2.2 Supersymmetry

Supersymmetry (SUSY) is a hypothetical symmetry between fermions and bosons. In this theory each standard model particle is associated with a super partner, which differs in the spin about $\frac{\hbar}{2}$. One version, where every fermion has two supersymmetric partners and every gauge boson one is called Minimal Supersymmetric Standard Model (MSSM). The theory provides solutions for some in the standard model appearing problems, for example the inclusion of the gravitation in a quantum field theory, the mass of the Higgs-boson and dark matter.

2.3 The ATLAS detector

The name ATLAS stands for "A Toroidal LHC ApparaturuS" and has a structure seen in figure 2. With a length of 46 m and a height of 25 m the whole detector has a weight of nearly 7×10^6 kg.

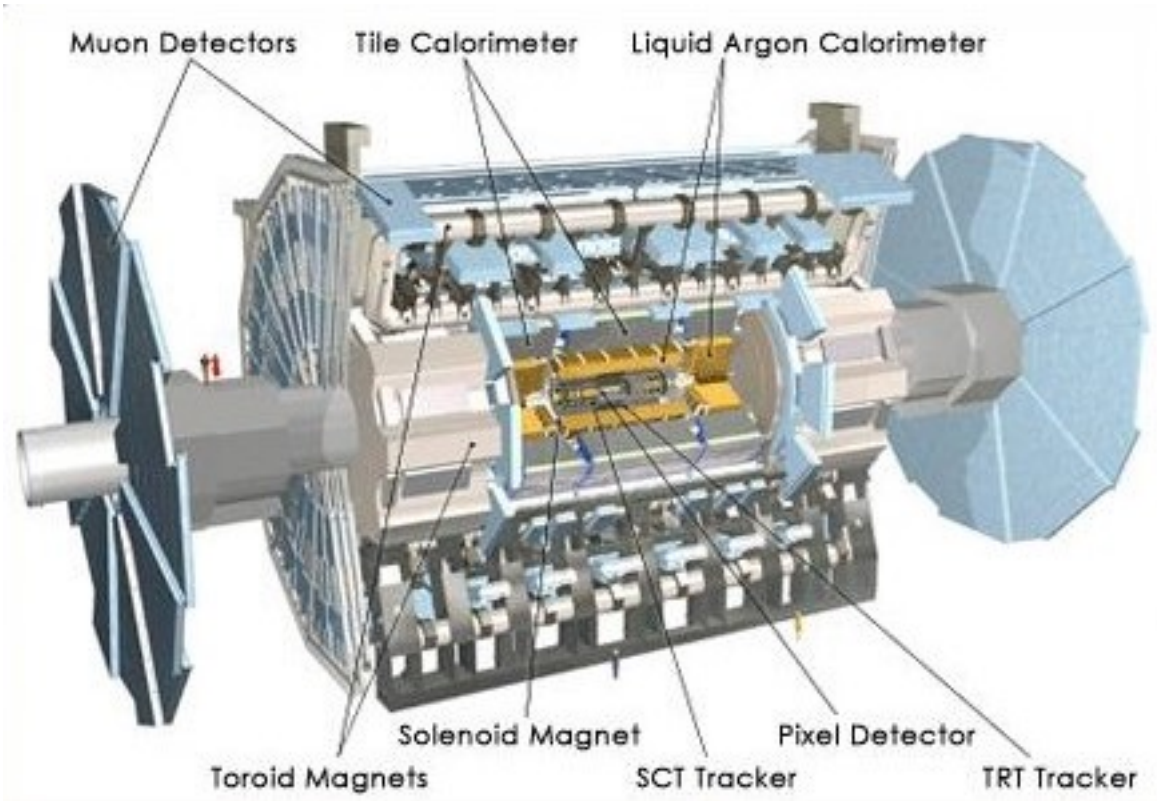

Figure 2: Schematically structure of the ATLAS detector [NYU].

2.3.1 Inner detector

The inner detector consists of four components:

- **Pixel detector** This component has a radial distance of 5 cm to 15 cm to the proton beam and measures the tracks of charged particles precisely. The detector is able to handle the electric signals of over 80×10^6 pixels. With the help of the pixel detector the primary interaction point is reconstructed as well as secondary vertexes.
- **Semi-conducted-tracker (SCT)** The SCT consists of long narrow stripes and also measures the tracks of charged particles.
- **Transition-Radiation tracker (TRT)** The TRT consist of small drift-chambers filled with gas. In this component the signal of the ionising particles is strengthened with transitions radiation.
- **Solenoid Magnet** The magnet is the last component of the inner detector and supplies a homogeneous magnetic field of B = 2 T in longitudinal direction. Due to the Lorentz force[4] the charged particles are bent in the magnetic field and therefore their transverse momentum can be measured. To get the bending radius of the particles we assume equality of the Lorentz force with the centrifugal force.

  $$e\left(\vec{v} \times \vec{B}\right) = \frac{m\vec{v}^2}{r} \tag{1}$$

  Now, for a known magnetic field strength and the measured track, we can obtain the transverse momentum with

  $$p[\mathrm{GeV}] = 0.3 \cdot B[\mathrm{T}] \cdot r[\mathrm{m}]. \tag{2}$$

2.3.2 Presampler

The presampler is the first detector component after the inner detector and supports the electromagnetic calorimeter within the measurement of the electromagnetic shower. Furthermore it is used to distinguish between one photon and a photon-pair out of π^0-decays.

2.3.3 Electromagnetic calorimeter (ECAL)

With the help of an electromagnetic calorimeter it is possible to identify electrons, positrons and photons as well as measuring their energy in a destructive process (compare figure 3). Therefor the effect that the mentioned particles produces electromagnetic showers, due to bremsstrahlung and pair production, is used. In the ATLAS detector a so called sandwich calorimeter is used, where layers in which the particle showers alternate with evidence layers (tracker chambers with liquid argon gas). Further an accordion design is used, which has advantages in read out performance. To be more precise, the layers are folded like an accordion and have a typically angle of 45° to the particle trajectory. Because of this, the particles passes much more material.

2.3.4 Hadronic calorimeter (HCAL)

The hadronic calorimeter is used to absorb and measure the energy of hadrons, which equivalent to electrons etc. produce electromagnetic showers, but also hadronic showers. The latter ones are more complex and wider. Therefore the HCAL consists of much more material than the ECAL, so that a complete absorption is guaranteed. With the HCAL it is for example possible to measure hadrons like protons and neutrons (compare the signatures in figure 3). Unlike the electromagnetic calorimeter the shower layers are made of iron and the evidence layers out of scintillator tiles and forward-fluid-argon-chambers.

[4] $F_L = q(\vec{v} \times \vec{B})$

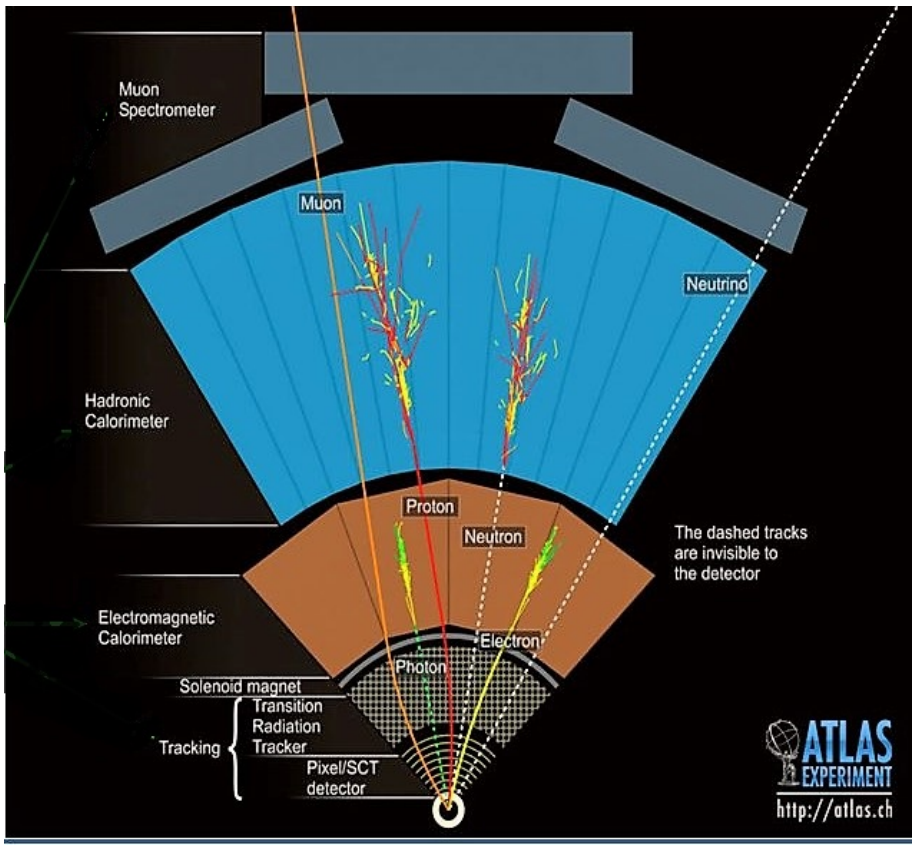

Figure 3: Particle signatures in the different components of the detector [Ned].

2.3.5 Muon system

The outermost part of the detector is the muon system, because muons indeed are charged leptons but due to its high mass do not form electromagnetic showers. Therefore muons pass the whole detector material and can only be observed with the help of the muon tracking chambers. The whole system occupies nearly half of the detector volume and has a separated magnetic system. Because of this an independent measurement of the momentum is possible.

3 Pre-lab questions

Decay of a Z^0-boson

To determine the momentum of a electron in the decay $Z^0 \rightarrow e^+e^-$, while the Z^0 is at rest, we start with the following equation:

$$P_{Z^0}^2 = (P_{e^+} + P_{e^-})^2$$

Now we are able to determine the energy via

$$\begin{aligned} M_{Z^0}^2 &= P_{e^+}^2 + P_{e^-}^2 + 2P_{e^+}P_{e^-} \\ &= M_{e^+}^2 + M_{e^-}^2 + 2\left(E_{e^+}E_{e^-} - |\vec{p_{e^+}}| \cdot |\vec{p_{e^-}}| \cdot \cos\theta\right) \\ &= M_{e^+}^2 + M_{e^-}^2 + 2\left(E_{e^+}E_{e^-} + |\vec{p}|^2\right) \end{aligned}$$

With $E_{e^\pm} << M_{e^\pm}$ wen can simplify that $E \approx |\vec{p}|$ and therefore get

$$\begin{aligned} M_{Z^0}^2 &= 4E_{e^+}E_{e^-} \\ \Leftrightarrow E^2 &= \frac{M_{Z^0}^2}{4}. \end{aligned}$$

With the Einstein energy relation and the known mass of $M_{Z^0} = 91.1876\,\text{GeV}$ we finally get

$$|\vec{p_e}| = \sqrt{\frac{M_{Z^0}^2}{4} - m_e^2} = 45.59\,\text{GeV}.$$

Scattering process $e^+e^- \to \tau^+\tau^-$

Asked is the momentum of the tau-leptons in the scattering process $e^+e^- \to \tau^+\tau^-$ in the centre-of-mass system with $s = 5\,\text{MeV}$ and a tauon mass of $M_\tau = 1.777\,\text{GeV}$.

$$\begin{aligned} s &= (P_{\tau^+} + P_{\tau^-})^2 \\ &= P_{\tau^+}^2 + P_{\tau^-}^2 + 2P_{\tau^+}P_{\tau^-} \\ &= M_{\tau^+}^2 + M_{\tau^-}^2 + 2\left(E_{\tau^+}E_{\tau^-} - |\vec{p_{\tau^+}}| \cdot |\vec{p_{\tau^-}}| \cdot \cos\theta\right) \\ &= 2M_\tau^2 + 2E_\tau^2 + 2|\vec{p_\tau}|^2 \\ &= 2M_\tau^2 + 2\left(M_\tau^2 + \vec{p_\tau}^{\,2}\right) + 2|\vec{p_\tau}|^2 \\ &= 4\left(M_\tau^2 + |\vec{p_\tau}|^2\right) \\ \Rightarrow |\vec{p_\tau}|^2 &= \left(\frac{s}{4} - M_\tau^2\right) \\ \Leftrightarrow |\vec{p_\tau}| &= \sqrt{\frac{s}{4} - M_\tau^2} \end{aligned}$$

With the given energy for s and M_τ it follows that

$$|\vec{p_\tau}| = 1.758\,\text{GeV}.$$

Determination of the transverse momentum of the W-boson

W-bosons decay mostly into hadrons ($q\bar{q}$ with 67.41 %), but also into charged leptons and their corresponding uncharged part (neutrino). For Example $e\nu_e$,$\tau\nu_\tau$ and $\mu\nu_\mu$ or jets. Therefore the transverse momentum can be defined by the conservation of the transverse four momentum:

$$P_{T,W} = P_{T,e} + P_{T,\nu}$$

Derivation of the Jacobi peak

We want to deduce the equation

$$\frac{\mathrm{d}\sigma}{\mathrm{d}p_T} = \frac{\mathrm{d}\sigma}{\mathrm{d}\cos\theta^*}\left|\frac{\mathrm{d}p_T}{\mathrm{d}\cos\theta^*}\right|^{-1} = \frac{\mathrm{d}\sigma}{\mathrm{d}\cos\theta^*}\frac{2p_T}{M_W}\frac{1}{\sqrt{\frac{1}{4}M_W^2 - p_T^2}} \tag{3}$$

from

$$\frac{\mathrm{d}\sigma}{\mathrm{d}\cos\theta^*} = 1 + \cos^2\theta^*.$$

For this we start with the expression for the transverse momentum which is given through:

$$\begin{aligned} p_T &= \frac{M_W}{2}\sin\theta^* = \frac{M_W}{2}\sqrt{1-\cos^2\theta^*} \\ \Leftrightarrow \cos\theta^* &= \sqrt{1-\frac{4p_T^2}{M_W^2}} \end{aligned} \tag{4}$$

To get equation 3 we differentiate the transverse momentum with respect to $\cos\theta^*$, and uses formular 4.

$$\begin{aligned} \frac{\mathrm{d}p_T}{\mathrm{d}\cos\theta^*} &= \frac{M_W}{4}\frac{-2\cos\theta^*}{\sqrt{1-\cos^2\theta^*}} \\ &= -\frac{M_W}{2}\frac{\cos\theta^*}{\sqrt{1-\cos^2\theta^*}} \\ &= -\frac{M_W^2}{4p_T}\sqrt{1-\frac{4p_T^2}{M_W^2}} \\ &= -\frac{M_W}{2p_T}\sqrt{\frac{M_W^2}{4}-p_T^2} \\ \Leftrightarrow \frac{\mathrm{d}\sigma}{\mathrm{d}p_T} &= \frac{\mathrm{d}\sigma}{\mathrm{d}\cos\theta^*}\left|\frac{M_W}{2p_T}\sqrt{\frac{M_W^2}{4}-p_T^2}\right|^{-1} \\ &= \frac{\mathrm{d}\sigma}{\mathrm{d}\cos\theta^*}\left|\frac{2p_T}{M_W}\frac{1}{\sqrt{\frac{M_W^2}{4}-p_T^2}}\right| \end{aligned}$$

Invariant four-lepton-mass

Because of the fact that the four lepton originate from a pair of real Z^0-bosons they have a minimal invariant mass of $2\mathrm{M}_{\mathrm{Z}^0}$[5]. However there can be events of four leptons with less energy, because there is a chance that one of the two Z^0-bosons is virtual.

Invariant four-lepton-mass from a Higgs decay

In this case we expected the maximum of the Breit-Wigner distribution around the mass M_H of the Higgs boson.

Missing transverse energy of a ideal and a real detector

In an ideal detector we expect a transverse missing energy of $\not{E}_T = 0$, since electrons and muons are completely identified. In a real detector on the other hand we have missing transverse momentum, because the complete momentum of a Z^0-pair might no be identified.

Branching ratio $t \to Wb$

A $t\bar{t}$-pair can decay in a final state with four charged leptons because of hadronization. The b quarks are able to hadronize in B-mesons which decay semi-leptonically. From this decay we get two additional leptons and therefore four leptons out of a $t\bar{t}$-event.

[5]Neglecting resolution effects of the detector.

4 Experimental Setup

The experiment can be divided into two parts. In the first part we use the ATLANTIS-event display to get an overview of the given data sets. With that the characteristics of the detector signatures for different events shall be learned. For this purpose learning sets for electrons, muons, tauons, photons and jets are given. Afterwards we look at the electron and the muon data set more precisely.

In the second part of the experiment we perform a so called electron calibration with the help of ROOT[6]. For this we use a provided C-file, which already contains a structure we have to follow and complete during the calibration. The calibration is required because of the fact that the atlas data only contains the raw energy, which is usually smaller than the true energy. Reason for this is for example dead material inside the detector, which is not sensitive on the deposited energy.

With the help of the calibration we are further measuring the W-boson-mass as the main goal of this lab course. For this several data sets are available. We have five ATLAS data sets available, two for the decay $W \to e\nu$ (one with our calibration and one without) and two for the decay $Z \to ee$ (one with our calibration and one without) and the data set we use for the electron calibration as explained above. Furthermore we have one Monte-Carlo data set[7] for the background and one with W-decay data for several W-masses available.

5 Assignments

5.1 Event displays

In the first part of the experiment we study the event displays of five different particles to get familiar with ATLANTIS. We choose one typical display for each, to point out the difference between them. These displays are shown in figure 4. The electron event display for example only shows a charged track and a entry in the ECAL (electromagnetic calorimeter) while the one for the muon shows also a charged track, but no entry in any of the calorimeters. Further in this case we have a signal in the muon chamber. So electrons and muons can be distinguished quite easily. The photon event displays are characterized by the fact that charged tracks cannot be observed while an energy deposition in the ECAL can. Tauons are special since their lifetime is so short, that they decay before they can be detected. The signals of the detector are showing the decay products which are for τ-leptons mostly 1-prong[8] or 3-prong[9] events. In general we see an energy deposition in the ECAL[10] and the HCAL[11] with at least one charged track for one tauon. In figure 4 a case with three tracks is shown. The last event display shows the jet data set and is characterized by multiple tracks which are due to hadronization effects.

In the following we choose Task 2 and Task 3 to process.

Task 2: Electron data set

In this task we are suppose to determine the momentum of the electrons with the help of the bending radius of the track. Since in the program the momentum is already calculated, we choose to do the reverse order and calculate the bending radius with the help of formula 2 (with a magntic field of $B = 2\,\mathrm{T}$ [Bon]). Further the energy deposition within the electromagnetic calorimeter is measured and the ratio of energy and momentum calculated. During this process events with three charged tracks are neglected. The values of the measured momentum and the energy in the ECAL are shown

[6] A software for data analysis based on C++ and developed at CERN.
[7] Simulated data.
[8] One charged particle plus neutral ones.
[9] Three charged particle plus neutral ones.
[10] For example from π^0-mesons.
[11] π^+ or π^-

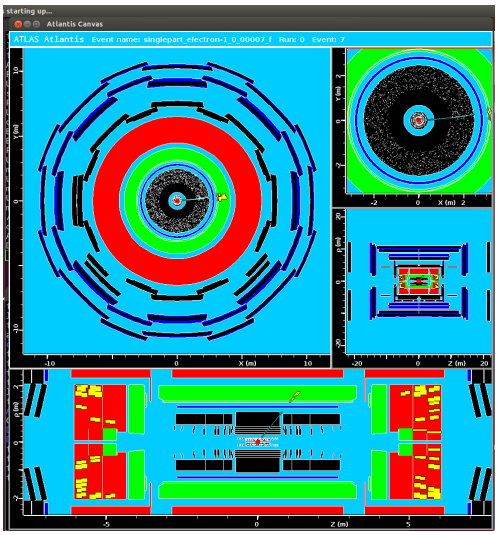

(a) Electrons

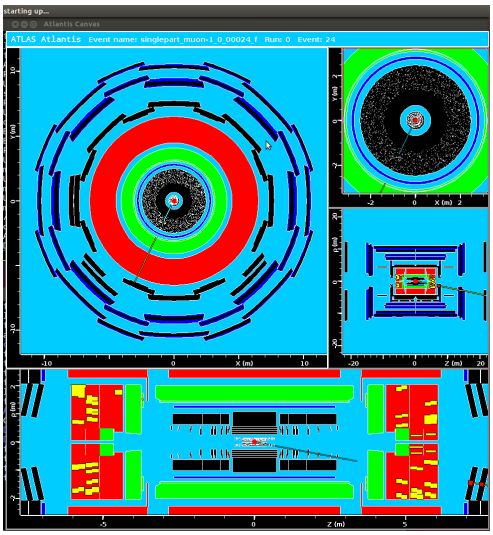

(b) Muons

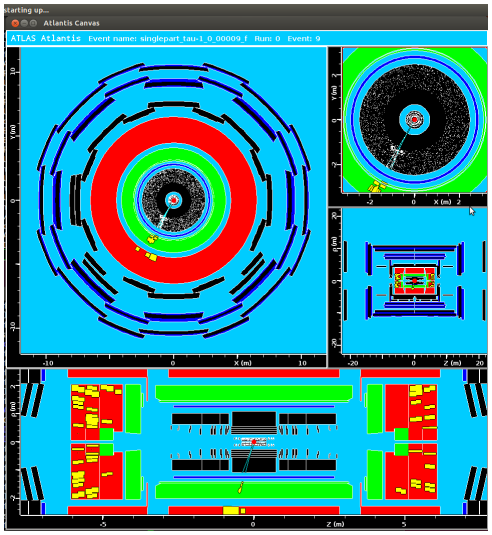

(c) Tauons

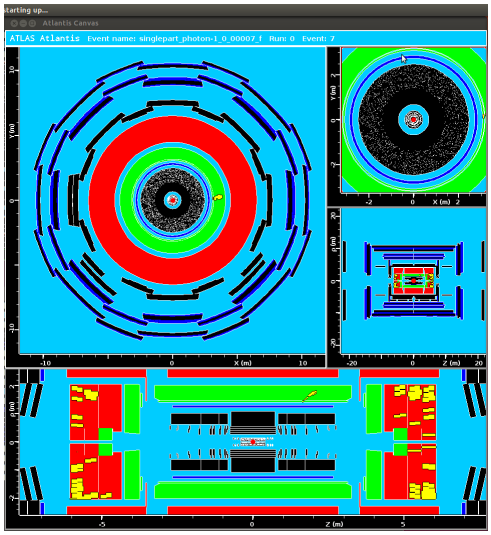

(d) Photons

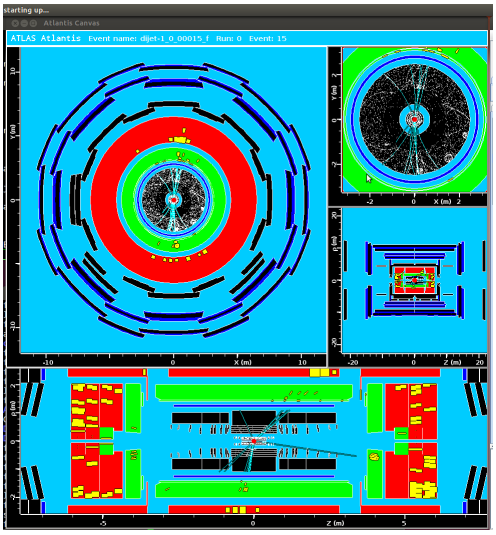

(e) Jets

Figure 4: Typical event displays for the five data sets.

Table 1: Data recorded from the electron data set. Afterwards the ration $|E/p|$ and the bending radius r is calculated.

event	p / GeV	E_ECAL / GeV	$\|E/p\|$	|r| / m
1	-26.20	54.7	-2.088	43.667
2	22.78	35.2	1.545	37.967
3	-244.35	223.2	-0.913	407.25
6	66.67	82.7	1.24	111.117
7	-7.55	56.6	-7.497	12.583
8	129.82	162.9	1.255	216.367
9	-3.27	51	-15.596	5.450
10	79.0	66.2	0.838	131.667
11	-95.93	79.5	-0.829	159.883
12	37.4	30.6	0.818	62.333
13	-89.35	36.5	-0.968	148.917
14	235.24	242.3	1.03	392.067
15	-105.14	105.3	-1.002	175.233
16	-50.35	139	-2.76	83.917
17	-28.62	28.1	-0.982	47.7
18	53.41	46.4	0.869	89.017
19	-32.92	64.3	-1.95	54.867
20	105.64	80.8	0.765	176.067
21	-34.3	153.3	-4.469	72.167
22	93.52	82.1	0.878	155.867
23	-113.98	97.8	-0.858	189.967
24	155.35	283	1.822	258.917
25	-36.4	33.8	-0.929	60.667
27	-55.46	48.8	-0.88	92.433
28	40.58	63.3	1.56	67.633
29	-100.09	90.3	-0.902	166.817
30	162.1	225.5	1.39	270.167
33	-69.17	49.2	0.711	115.283
34	64.03	53.9	0.842	106.717
35	-13.18	36.6	-2.78	21.967

in table 1 as well as the ratio and the bending radius we determined. We also generate a histogram of the absolute value of the calculated ratio (compare figure 5). Since we know that $\left|\frac{\mathrm{E}}{\mathrm{p}}\right| \approx \left|\frac{\mathrm{c}}{\mathrm{v}}\right|$ we would expect values greater than one, because particles should not be able to travel faster than light. In our case we have the most values between 0.5 and 1. Still, this observation is possible because of the fact that we don't have an ideal detector. In real detectors the particles can loose energy between the measurement of the momentum (which takes place at first) and the measurement of the energy loss (which takes place later) unnoticed[12]. If this happens we would have measured less energy than the measured momentum let us assume.

Task 3: Muon data set

In contrast to task 2 we now measure the momentum within the inner detector and within the muon chamber. Afterwards we compare them to each other. Further we determine the energy loss in the

[12]For example because of non-sensitive material.

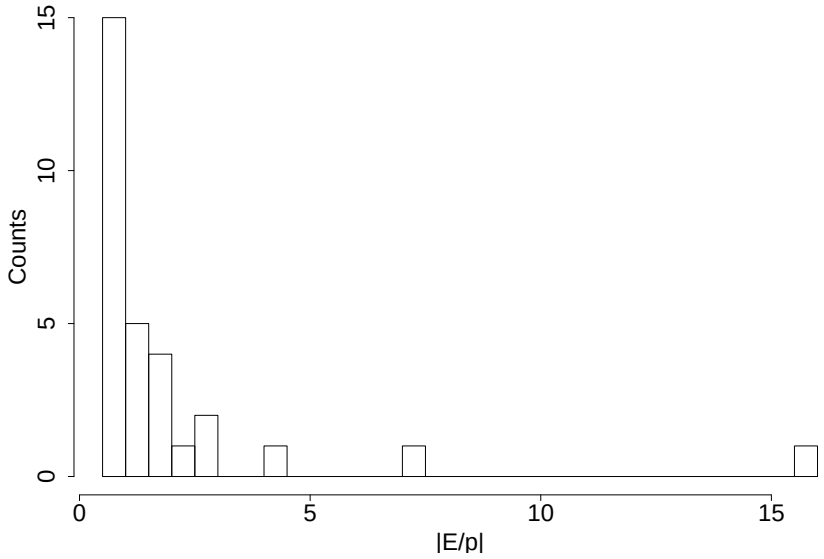

Figure 5: Histogram of the absolute ratio $\left|\frac{\mathrm{E}}{\mathrm{p}}\right|$.

calorimeters and examine which factor has the biggest influence on it. The measured values for this task are shown in table 2. Looking at the values it can be seen that for some events (e.g. event 14) the momentum of the electron increases while its passes the detector. This is physically not possible (particles loose energy while passing matter), but if detector effects are considered, we can reduce this observation back to detector resolution. The resolution creates a gaussian distribution around the particle momentum. It further becomes asymmetric, since it is always possible to loose momentum, but not to gain some. Depending on the position of the muon in these distributions (first and second momentum measurement) an momentum increase is possible. Looking at the values listed in the table, we also recognize a much higher entry in the calorimeters for the last event than for the others. A reason for this could be. that for this event we not just measured the energy deposition, but also the noise in the outer hadron calorimeter. Beside this we are not able to see a coherence between the energy loss and for example the variables ϕ or η and therefore come to the conclusion that the energy loss shows an isotropic behaviour. The energy deposition on average is given by 2.01 GeV, with neglecting the last value.

5.2 Energy calibration of the electrons

In this part we want to calibrate the electron energy as announced in section 4. For the calibration we use electron-positron-pairs which originate from Z^0-decays, measured precisely at the LEP-storage ring. For this purpose we first create histograms for the electron and positron energy (compare figure 6) by using the `tree− >draw` command of root. Because of the fact that the pairs originate from a Z^0-decay we expect the peaks of both histograms at an approximate energy of half of the Z^0 mass ($\sim 45\,\mathrm{GeV}$), which we can confirm in both cases.

For the calibration we look at the distribution of the invariant electron-positron-mass, which should peak at the Z^0 mass (theoretical value is $(91.1876 \pm 0.0021)\,\mathrm{GeV}$ [Bon]). Using a so called Voigt function, which is a convolution of the Breit-Wigner function with a Gauss, it is possible to fit the distribution and determine important parameters as peak (mass) and width[13] (resolution). In figure 7 we plot the histogram of the invariant mass and the corresponding fit, without any calibration. Here we can make two observations. First that the fit without improvements delivers quite a low value for the peak and with that for the Z^0 mass ($M_{Z^0} = (85.57 \pm 0.04)\,\mathrm{GeV}$). Second that the distribution

[13] Actually it is not the normal width, but a width corresponding to the resolution (gaussian function).

Table 2: Data recorded from the muon data set. The momentum in the inner and in the muon detector as well as the energy deposition in both calorimeters (CAL) are determined.

event	p_{in} / GeV	p_{out} / GeV	E_CAL / GeV	η	ϕ / °
1	-85.28	-53.92	2.7	1.437	21.008 ± 0.009
2	43.40	43.83	1.6	-0.767	24.877 ± 0.009
3	-241.37	-237.02	0	-2.438 ± 0.001	230.107 ± 0.017
4	48.89	44.77	2.8	0.567 ± 0.001	311.119 ± 0.007
5	-168.16	-177.62	0	-1.809	244.395 ± 0.008
6	117.32	96.56	1.7	1.621	151.865 ± 0.009
7	-71.94	-64.96	2.4	0.699 ± 0.001	3.804 ± 0.006
8	199.91	199.44	1.3	1.797	67.324 ± 0.008
9	-57.84	-50.01	3	-0.287 ± 0.001	240.986 ± 0.005
11	-100.75	-94.11	1.4	-1.636 ± 0.001	48.016 ± 0.012
12	38.26	34.48	2.5	0.189 ± 0.001	326.10 ± 0.06
13	-105.19	-108.68	3.2	1.163 ± 0.001	223.748 ± 0.006
14	236.12	263.61	2.1	2.286 ± 0.001	103.025 ± 0.013
15	-131.69	-125.51	2.8	-1.763	254.894 ± 0.009
16	152.24	157.69	3.8	-1.874	27.045 ± 0.009
17	-35.23	-32.18	2.2	0.395 ± 0.001	326.388 ± 0.007
18	54.19	50	2.7	0.229 ± 0.001	336.212 ± 0.005
19	-84.75	-68.09	1.7	0.773	259.873 ± 0.006
20	104.26	107.98	2.3	1.421	77.622 ± 0.007
21	-184.01	-170.66	21.8	-2.329 ± 0.001	25.237 ± 0.016

has a high width (bad resolution). Therefore we have to calibrate the electron energies to get a better result.

For the energy calibration have to do some assumption. Normally we would expect that the quantities used in the calibration are correlated. This means that the correction for example for the energy not just depends on the energy range itself, but also on the position of the deposition in the detector (ϕ and η). Since in this task just the idea of such a calibration shall be given, there is no time to consider such dependencies[14]. So we assume that every quantity has a correction factor independently of the others. The data file ElecCalib.C we produce while calibrating the electron energy is shown in figure 8. To create this data file we first look at the variable η (pseudo-rapidity) and afterwards at the azimuthal angle ϕ. For the variable η we observe a huge dependence, so we correct our values in steps of 0.5 from -2.5 to 2.5. For each area we look at the fitted data and multiply the energy in ElecCalib.C with the ratio between the energy given by the fit and the real Z^0 energy. After this corrections our fit of the electron calibration becomes much better than before (compare figure 13(a) in the appendix), although the fitted peak is still to low. To further correct this we use the variable ϕ from $-180°$ to $180°$ in steps of $\pi/4$. This gives us the electron correction in figure 13(b) in the appendix. Because of the fact that the calibration is still improvable, we try to use the raw energy for further corrections. Looking at figure 13(c) in the appendix it can be seen that this corrections has some problems. One one hand the width is smaller, what is good in terms of resolution, but the Voigt function fails to describe the distribution properly. After we restrict the fitting borders using the fit panel of ROOT the fit performs well, but shows that the Z^0 mass is reconstructed too high. Therefore we decide not to take the raw energy into account. In figure 9 the final result can be seen, where the raw energy before the electron calibration is illustrated by the blue curve and the energy after the calibration by the green one. Now our Z^0-mass is given by $M_{Z^0} = (91.11 \pm 0.03)\,\text{GeV}$ with

[14] Too many combinations.

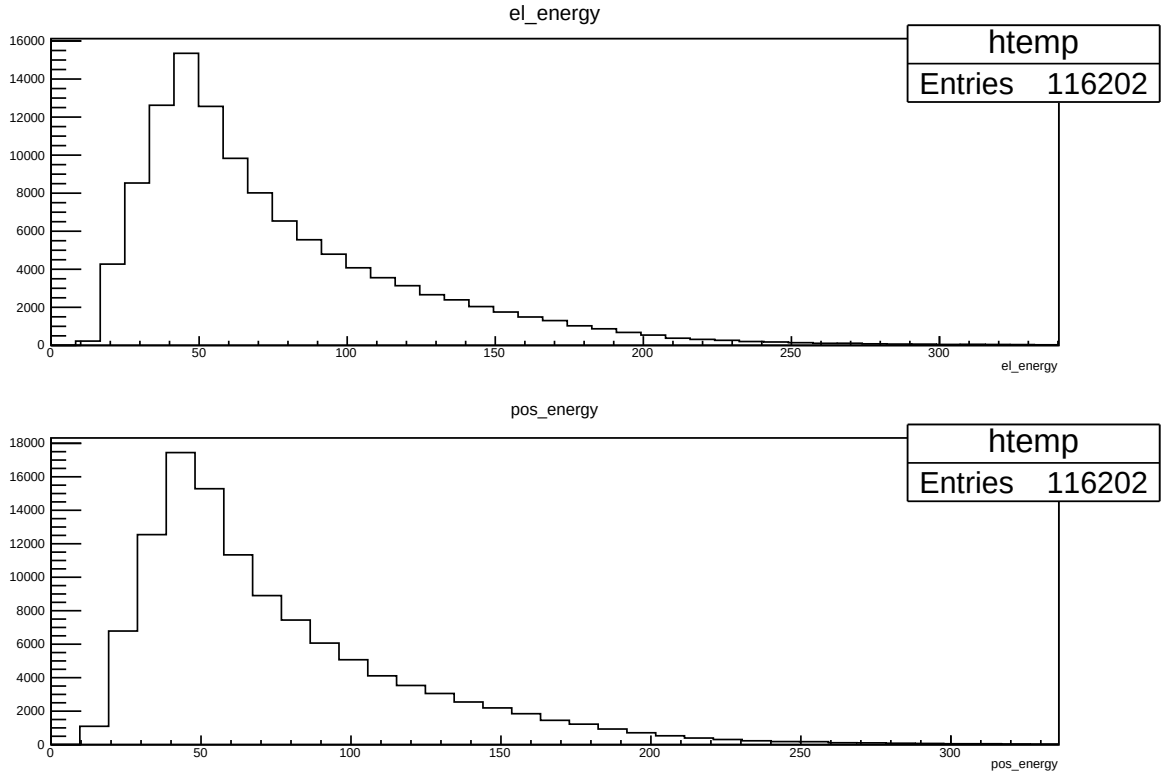

Figure 6: Histograms of the electron (upper picture) and positron (lower picture) energy.

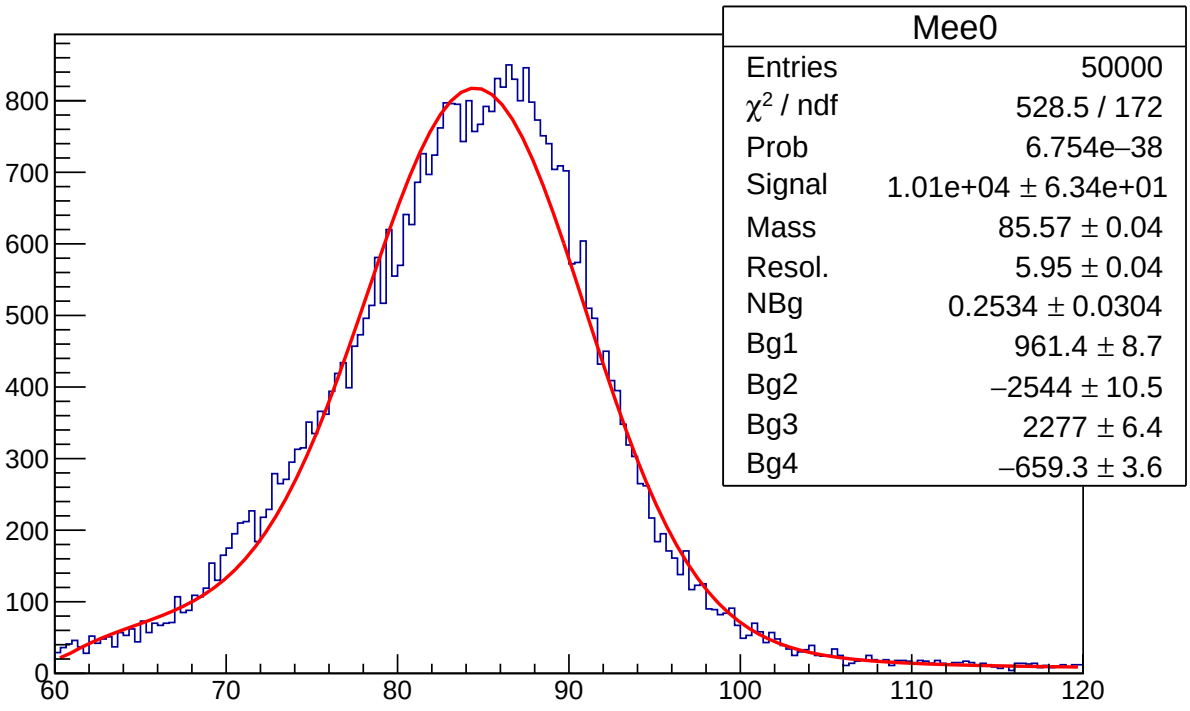

Figure 7: Histogram of the invariant electron-positron-mass without any calibration.

a resolution of (3.941 ± 0.003) GeV and a χ^2/ndf of 1.901. The χ^2 ideally should be around 1, so we are a little bit to high, however our fit looks quite good and the energy is much better than before.

```
#include "math.h"
#include "TMath.h"

double ElecCalib(double e_raw, double pt, double eta,
                 double phi, double etiso, double eoverp, double mindrjet)
{
  double dummy=pt*eta*phi*etiso*eoverp*mindrjet;
  double energy = e_raw;

  //Correction depending on eta range
  if (eta>-2.5 && eta<-2) energy = energy * 91.2/76.87;
  else if (eta>-2 && eta<-1.5) energy = energy * 91.2/81.3;
  else if (eta>-1.5 && eta<-1) energy = energy * 91.2/84.72;
  else if (eta>-1 && eta<-0.5) energy = energy * 91.2/87.26;
  else if (eta>-0.5 && eta<0) energy = energy * 91.2/88.96;
  else if (eta>0 && eta<0.5) energy = energy * 91.2/88.85;
  else if (eta>0.5 && eta<1) energy = energy * 91.2/87.51;
  else if (eta>1 && eta<1.5) energy = energy * 91.2/85.33;
  else if (eta>1.5 && eta<2) energy = energy * 91.2/81.82;
  else if (eta>2 && eta<2.5) energy = energy * 91.2/78.02;

  //Correction depending on phi range
  phi = phi*180/TMath::Pi();
  if (phi>-180 && eta<-135) energy = energy * 91.2/90.95;
  else if (phi>-135 && eta<-90) energy = energy * 91.2/90.85;
  else if (phi>-90 && eta<-45) energy = energy * 91.2/90.79;
  else if (phi>-45 && eta<0) energy = energy * 91.2/90.65;
  else if (phi>0 && eta<45) energy = energy * 91.2/90.98;
  else if (phi>45 && eta<90) energy = energy * 91.2/91.02;
  else if (phi>90 && eta<135) energy = energy * 91.2/90.67;
  else if (phi>135 && eta<180) energy = energy * 91.2/90.82;


 // Correction depending on energy range
 //if (e_raw>0 && e_raw<50) energy = energy * 91.2/92.07;
 //else if (e_raw>50 && e_raw<100) energy = energy * 91.2/91.85;
 //else if (e_raw>100 && e_raw<150) energy = energy * 91.2/88.2;
 //else if (e_raw>150 && e_raw<200) energy = energy * 91.2/85.87;
 //else if (e_raw>200 && e_raw<250) energy = energy * 91.2/85.22;

  return energy;
}
~
~
~
```

Figure 8: ElecCalib.C after the successful energy calibration.

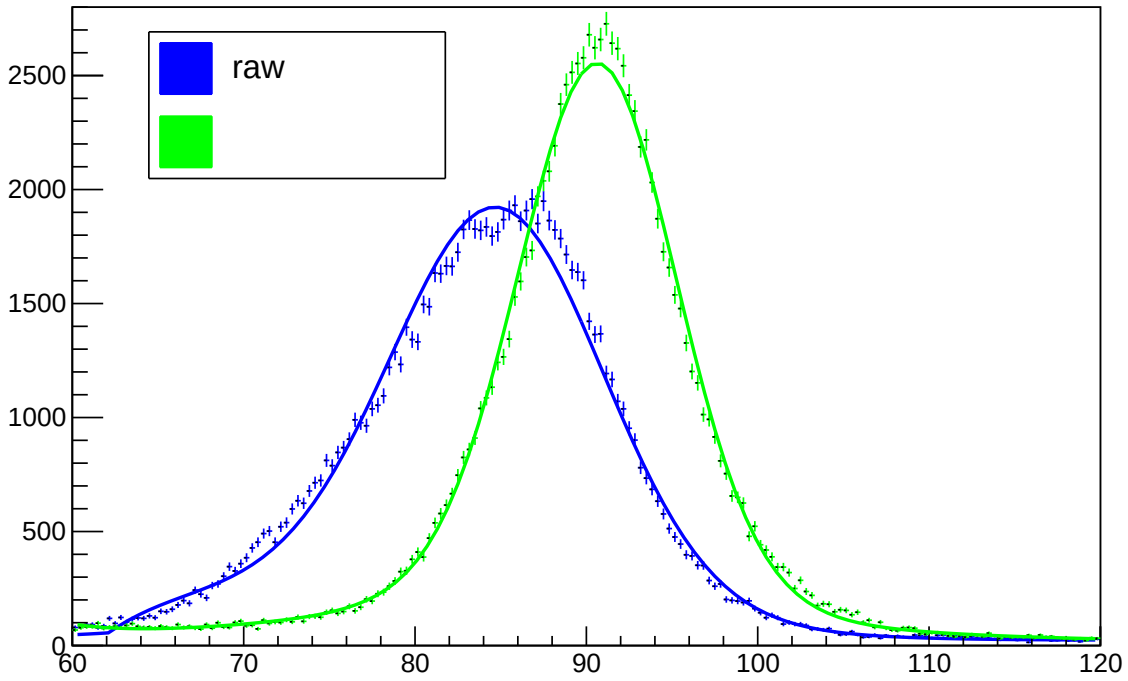

Figure 9: Comparison of the electron calibration before our changes and after.

5.3 Measurement of the W-boson mass

To measure the mass of the W-boson formula 3 is used. If the transverse momentum of the electrons is plotted, a singularity called Jacobi peak can be seen at a position, which equals half of the W mass. Due to resolution effects, in reality we don't see a singularity but something that is smeared out[15]. The best way to determine the position of this Jacobi peak in the smeared out distribution is, to fit a polynomial to the steep right side of the distribution. From that the so called half maximum (HF) can be determined, which should be equal to half of the W mass.

For the Measurement of the W-Boson-mass several data sets are available:

- ATLAS data set with $W \to e\nu$ with our calibration applied on
- ATLAS data set with $W \to e\nu$ without our calibration applied on
- ATLAS data set with $Z \to ee$ with our calibration applied on
- ATLAS data set with $Z \to ee$ without our calibration applied on
- $Z \to ee$ data set we used for the electron calibration
- Monte-Carlo-data set with W-decay ($W \to e\nu$) simulated for different W-masses (79 GeV, 79.5 GeV, 80 GeV, 80.5 GeV and 81 GeV)
- One data set with Monte-Carlo-background

To begin with we create histograms with the command `tree− >draw` for the number of jets, the electron momentum p_T and the W transverse momentum ptw, both for the W-ATLAS data set and

[15]Similar as if the singularity would be convoluted with a gaussian curve.

one Monte-Carlo-simulated data set (we choose the energy of 80.5 GeV) to get a first overview. The histograms for ATLAS are shown in figure 10(a) and the ones for the Monte-Carlo data in figure 10(b). Comparing them, the first thing noticed is that the ATLAS data set has twice as many entries as the Monte-Carlo-data. Further the tail of the histogram of the electron momentum as well as the tail of the histogram of the transverse momentum is in the simulated data not that pronounced.

Afterwards we plot the W-Boson ptw-spectrum of the ATLAS data set for jet numbers from zero to four (compare figure 11). For njet = 0 we get the most entries and the most narrowly histogram. The reason for this is the fact that the W-boson with a jet number of zero are generated from hadron collisions as described in first order collisions. Higher orders of the jet numbers mean a higher recoil and with that a higher transverse momentum.

5.3.1 Applying cuts

To be able to do a meaningful measurement of the W-boson-mass we have to apply cuts to select useful events of the data sets. For the cuts we look at the variables `njets`[16], `ptw`[17] and `etmis`[18]. The cut for `njets` we will extract from figure 11, for `etmis` from 14(a) in the appendix and for `ptw` from 14(b) in the appendix. The aim of the cutting process is a sharper Jacobian peak to get a better W mass measurement, which for example can be reached with small transverse momentum of the W-boson.

- `njet`: We want as less transverse momentum (unequal to zero) and as much events as possible for the W-bosons. Therefore we set our cut to $\texttt{njet} \leq 1$.
- `etmis`: We want to cut on an area were we don't have too much or to less missing energy, since we expect some from the neutrino but not too much. We choose $20 < \texttt{etmis} < 70$.
- `ptw`: As already mentioned we want as less transverse momentum as possible for the W-bosons. So for the last cut we choose $\texttt{ptw} < 20$.

Looking at our cutting process based on the histogram of `el_pt`[19] (compare figure 15 in the appendix) it is obvious that the Jacobian peak is sharper than before. Now we are able to apply the cuts on our seven data sets.

5.3.2 Calibration curve

After applying the cuts to our data sets we are able to determine the W-boson mass. Therefor we look at first at the calibrated Monte-Carlo data sets for the five different W masses and plot the determined half maximum (position of the Jacobi peak) of each as a function of the Monte-Carlo mass. The graphs from which we extract the values for the half maximum are shown in figure 16 in the appendix. The values can be seen in table 3. Our calibration curve is shown in figure 12 and the

Table 3: Determined half maximum for the Monte-Carlo simulated W-mass.

M^W_{sim} / GeV	half maximum / GeV
79.0	41.92 ± 0.55
79.5	42.16 ± 0.15
80.0	42.54 ± 1.40
80.5	42.81 ± 1.30
81.0	43.15 ± 0.10

[16] Number of charged tracks.
[17] Transverse momentum.
[18] Missing energy.
[19] Transverse momentum of the electron.

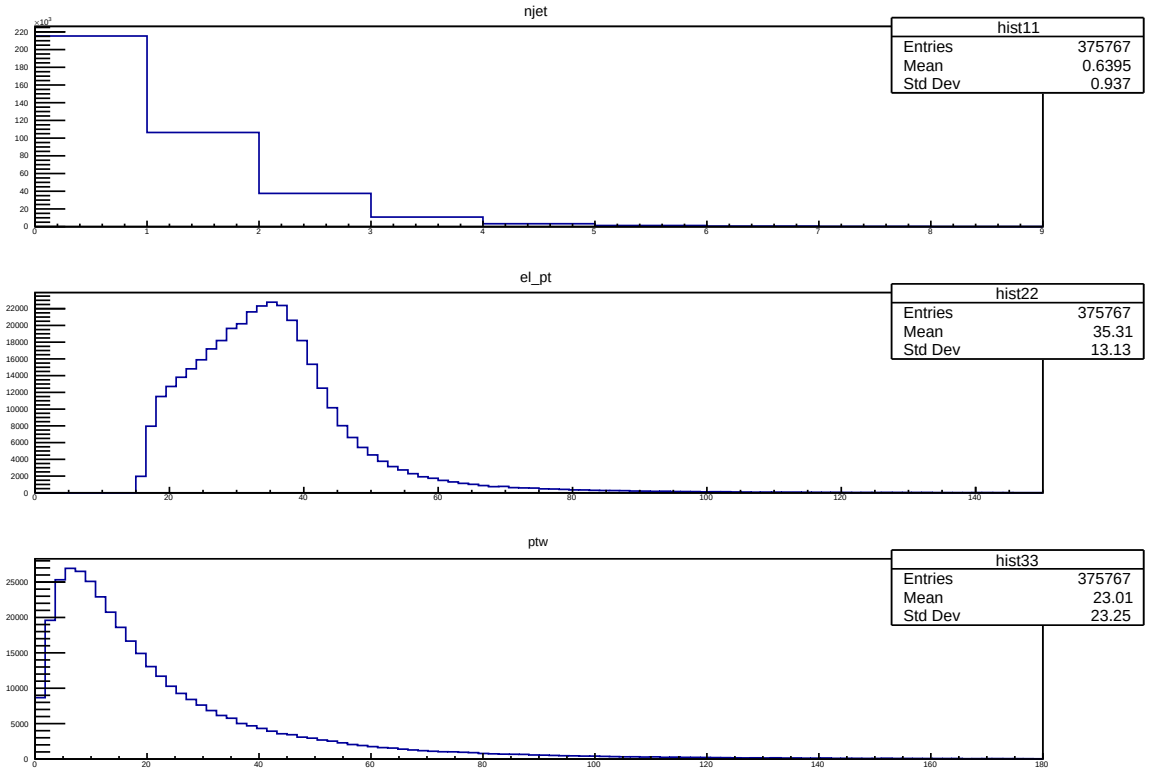

(a) ATLAS data set

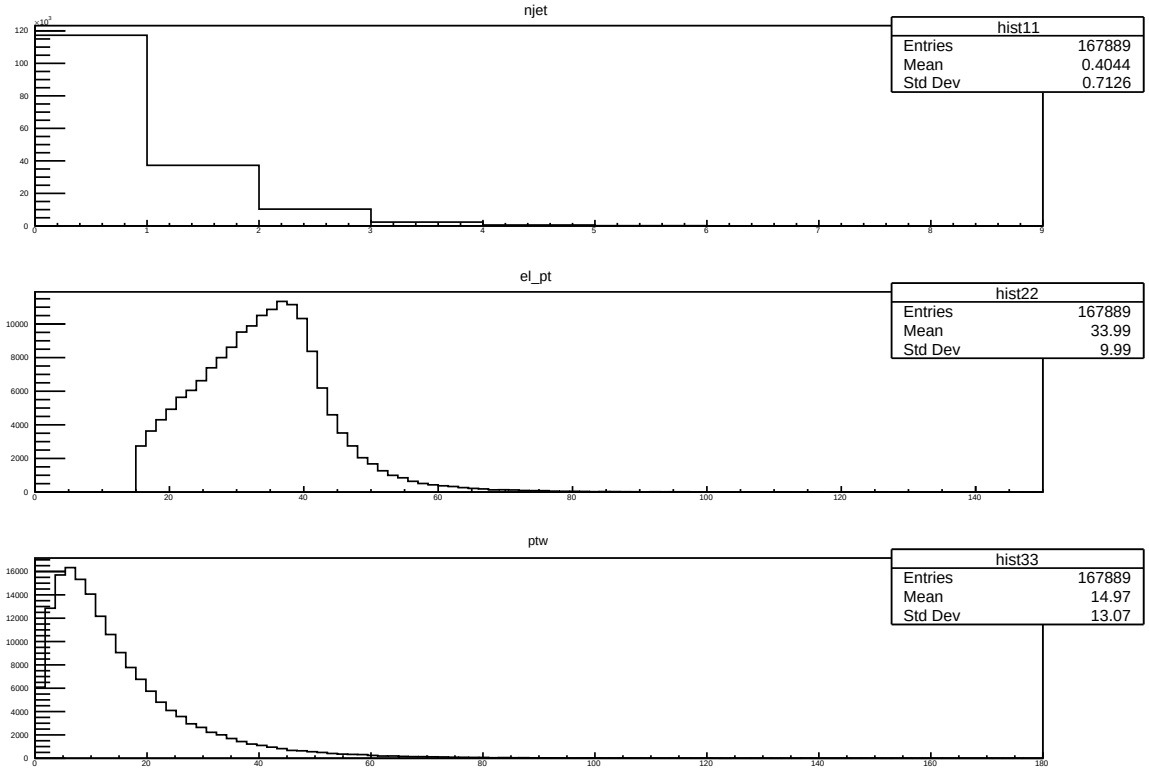

(b) Monte-Carlo-simulated

Figure 10: Histograms for the ATLAS and the Monte-Carlo-simulated data sets.

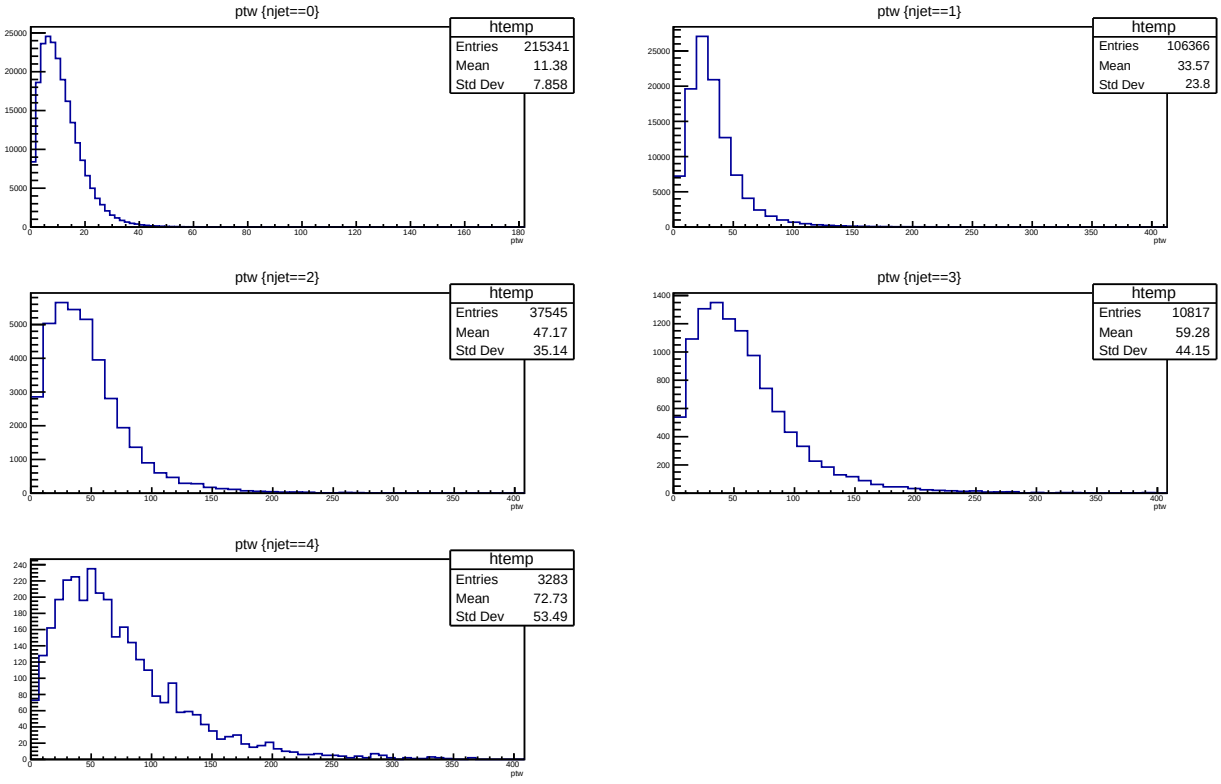

Figure 11: W ptw-spectrum for the ATLAS data set for different jet numbers.

fitted linear function is given by

$$\mathrm{HM} = (0.65403 \pm 0.01034) \cdot \mathrm{M}_W - (9.82725 \pm 0.83230)\,\mathrm{GeV}. \tag{5}$$

The reduced χ^2/ndf of the fit has a value of 0.00823.

Now if we measure the position of the Jacobi peak from the Atlas data set for the decay $\mathrm{W} \to e\nu$, we can use the calibration curve to determine the proper calibrated mass. In case of the ATLAS data set we first subtract the Monte-Carlo background to correct the measured events. For this we try to use the function `AddHistograms()` [Bon] (page 73), but this does not work. Therefore we use a different method to subtract the background. Furthermore by looking at the $\mathrm{Z} \to ee$ data set with and without our energy calibration from section 5.2, it is obvious that our calibration ensured, that the maximum is shifted to the right position (figure 17 in the appendix). This shows that without the calibration of the raw energies our W-boson mass would be way off and that this correction was necessary.

From figure 18 (Atlas data set with substracted background) we are able to extract the half maximum to $\mathrm{HM_W} = (42.54 \pm 19.00)\,\mathrm{GeV}$. To be able to determine the W-boson mass we use the fit-function in equation 5 and reorganize it to

$$\mathrm{M_W} = \frac{\mathrm{HM} + (9.82725 \pm 0.83230)\,\mathrm{GeV}}{(0.65403 \pm 0.01034)}$$

$$\sigma_{\mathrm{M}_W} = \sqrt{\left(\frac{\sigma_{\mathrm{HM}}}{0.65403}\right)^2 + \left(\frac{\mathrm{HM} \cdot 0.01034}{0.65403^2}\right)^2 + \left(\frac{0.8323\,\mathrm{GeV}}{0.65403}\right)^2}$$

With this we finally get a W-boson mass of

$$\mathrm{M_W} = (80.069 \pm 1.662)\,\mathrm{GeV}$$

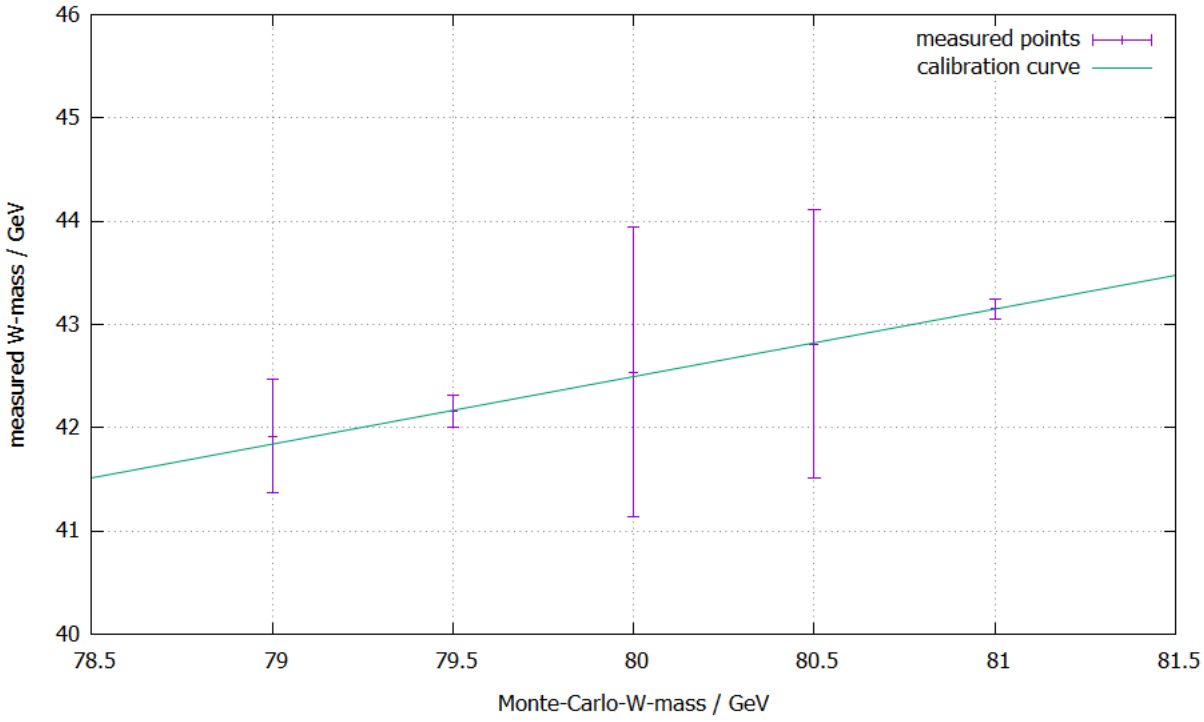

Figure 12: Calibration curve to determine the W-boson mass.

which lies in the one-sigma area of the theoretically value ($M_W^{theo} = (80.403 \pm 0.029)$ GeV [Bon]). If we hadn't subtract the background, we would have get a half maximum of $HM_{without} = (42.47 \pm 0.24)$ GeV (compare figure 19 in the appendix) and with that a boson mass of $M_{W,without} = (79.962 \pm 1.676)$ GeV. This shows that it was really necessary to take the background into account.

6 Discussion

The aim of the experiment was (because we chose assignment 3) to determine the W-boson mass out of a real ATLAS data set. During the first part of the experiment, event displays were studied with the help of ATLANTIS, to learn how to distinguish between different particle signatures in the detector. This went really well with no problems. Afterwards we were calibrate the raw energy of the electrons with a given data sheet called ElecCalib.C. This was also done with success.

In the second part the mass of the W-boson was determined. It became obvious how important the first part was to get the best result possible. Our final result of $M_W = (80.069 \pm 1.662)$ GeV is, compared to the theoretically value, quite good. To be precise, we only have a difference of 0.334 GeV to the theoretical value, which we can cover easily with our error.

7 Appendix

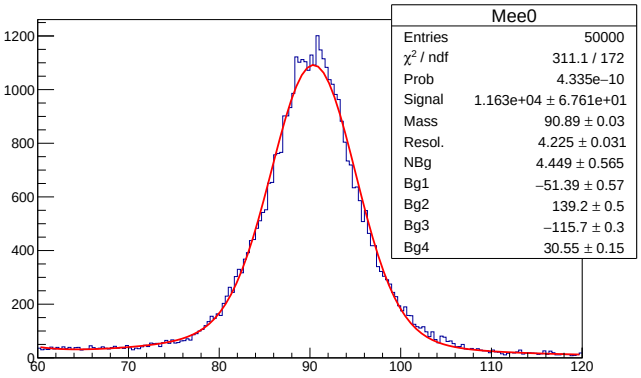

(a) Electron calibration with regard to η.

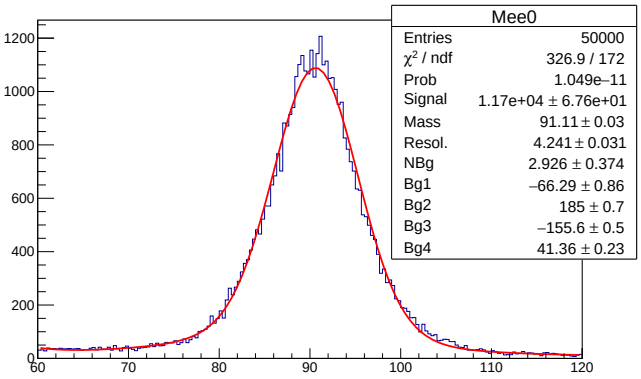

(b) Electron calibration with regard to η and ϕ.

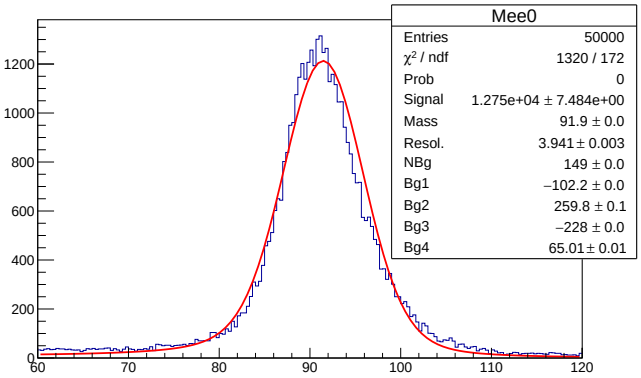

(c) Electron calibration with regard to η,ϕ and the raw energy

Figure 13: Electron calibration.

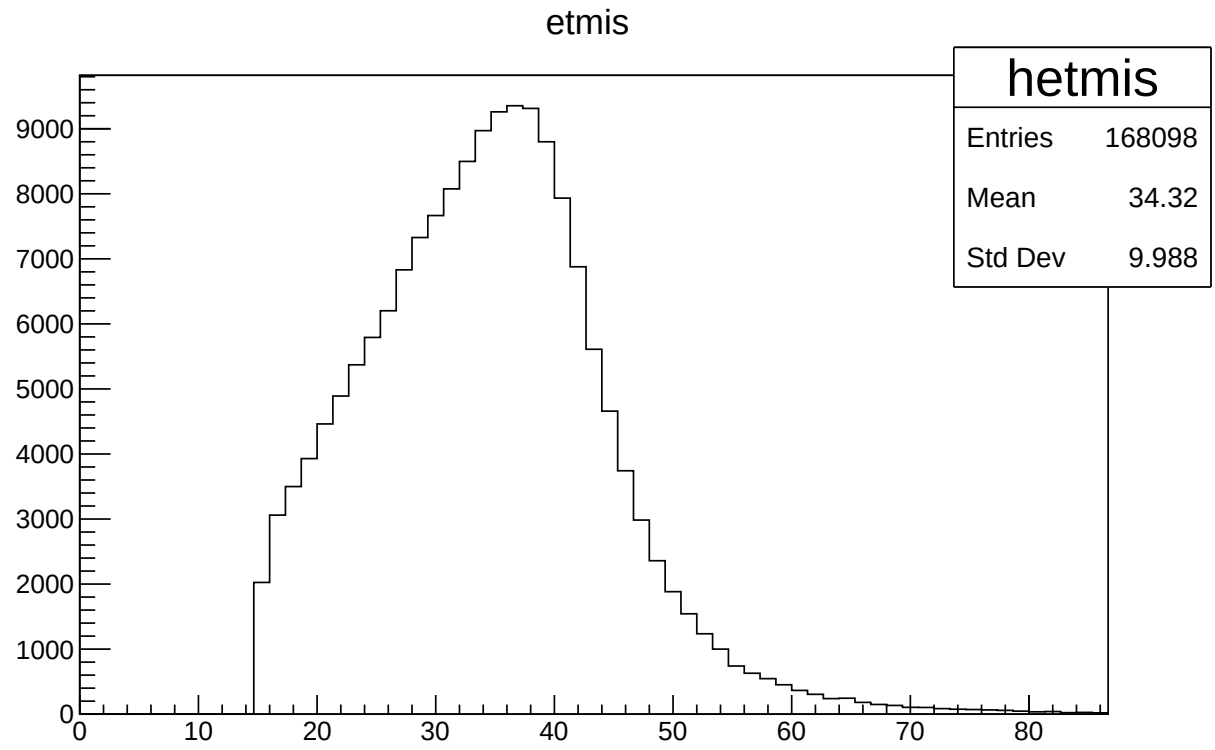

(a) `etmis`.

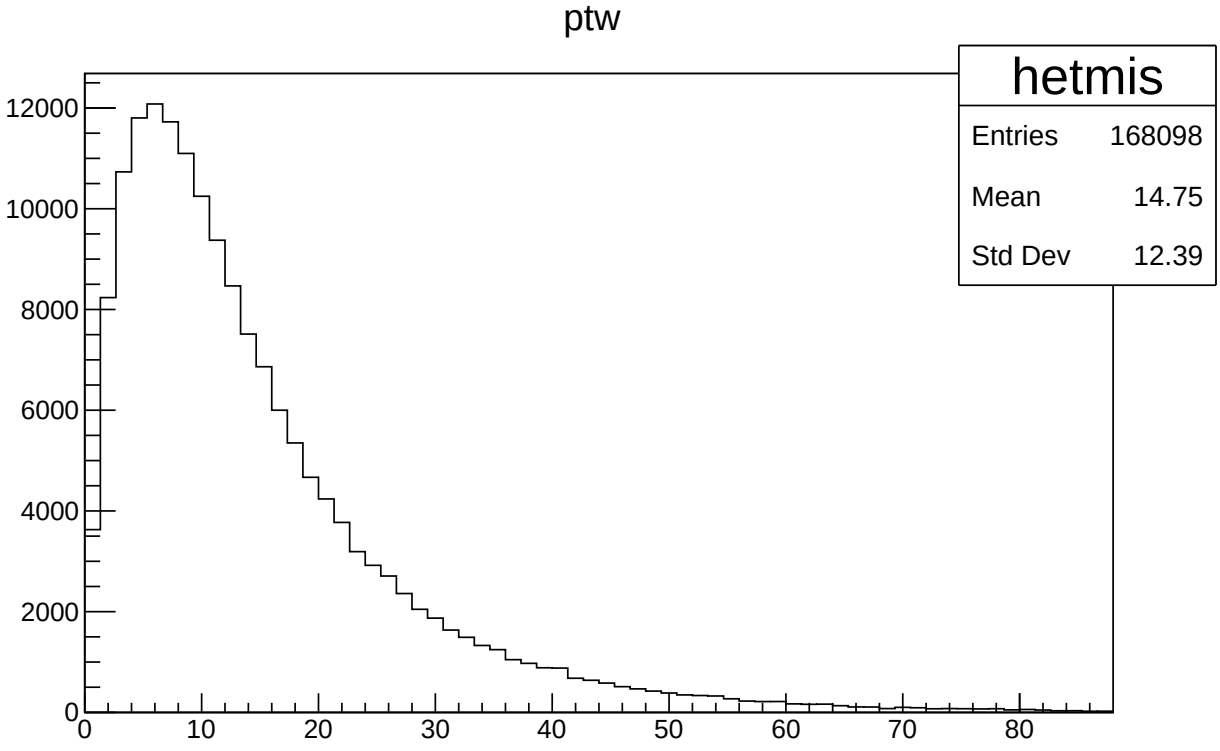

(b) `ptw`.

Figure 14: Histograms we extract the cuts for `etmis` and `ptw` from.

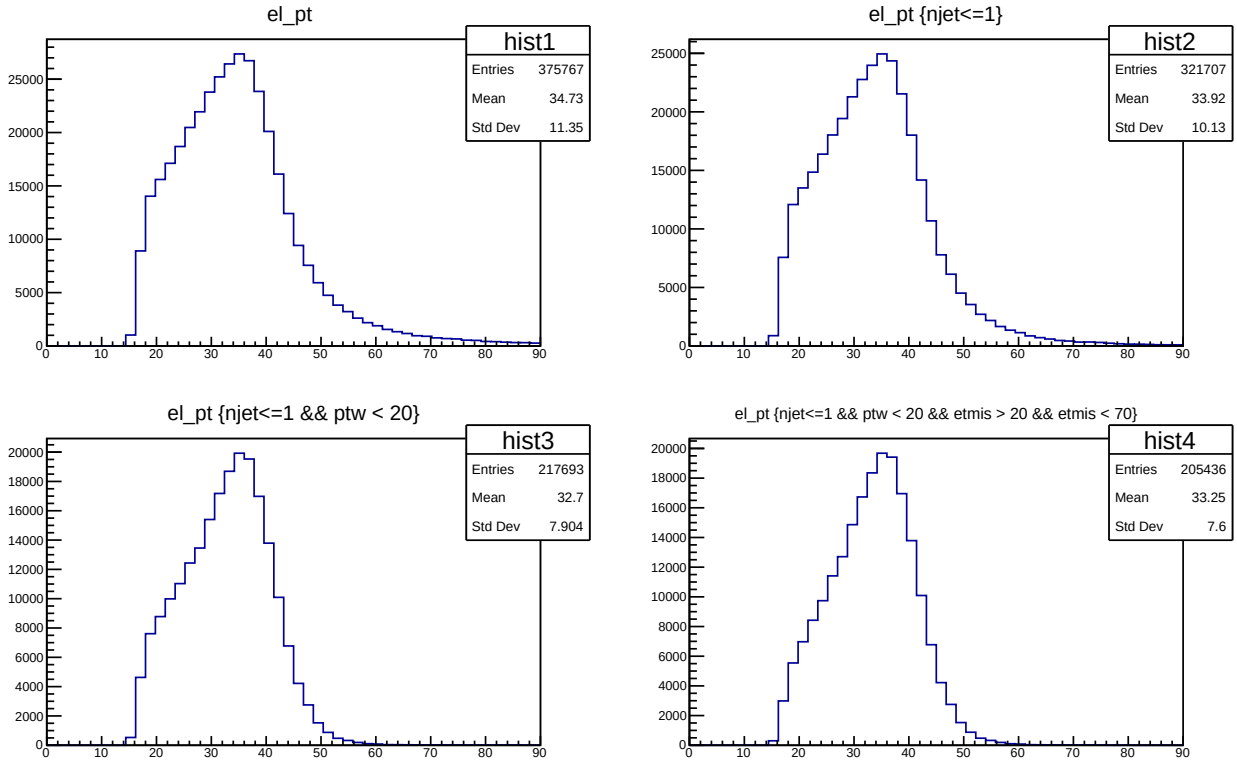

Figure 15: Cutting process with the ATLAS data set for $W \to e\nu$.

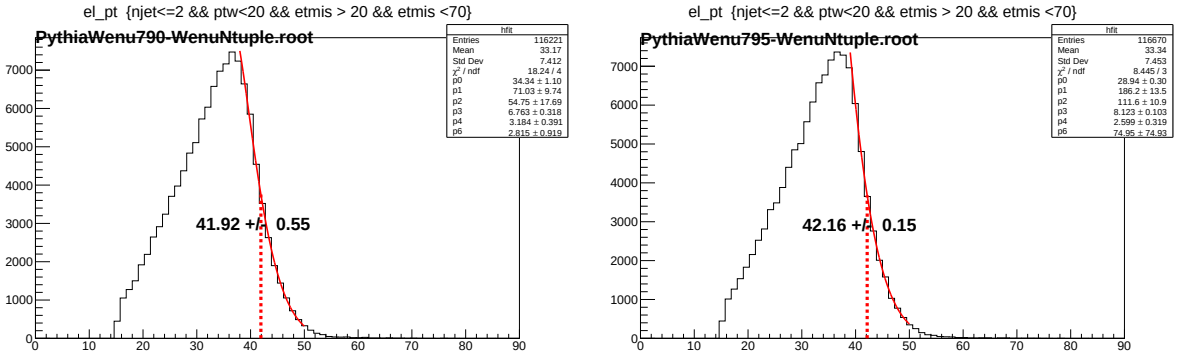

(a) $M_{sim,79\,GeV}$

(b) $M_{sim,79.5\,GeV}$

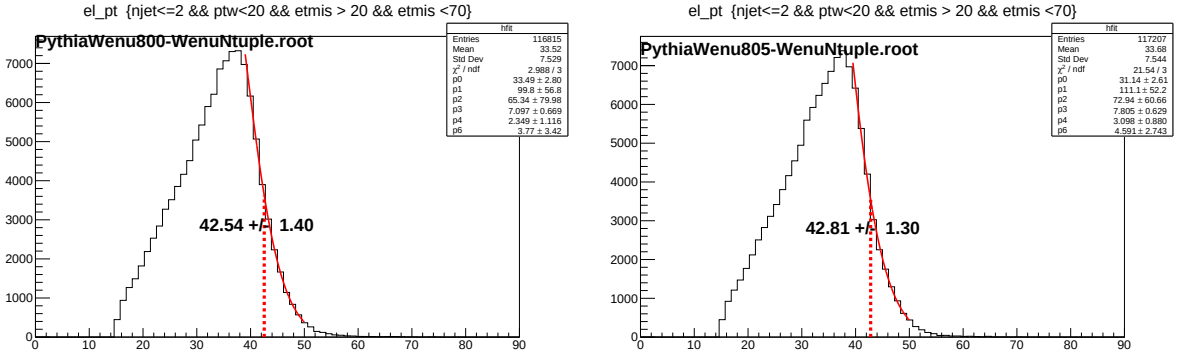

(c) $M_{sim,80\,GeV}$

(d) $M_{sim,80.5\,GeV}$

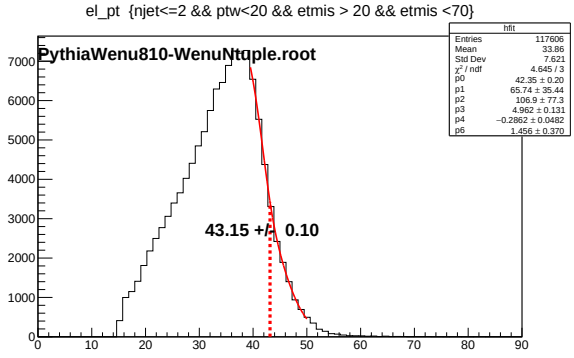

(e) $M_{sim,81\,GeV}$

Figure 16: Half maximum of the Monte-Carlo-simulated data.

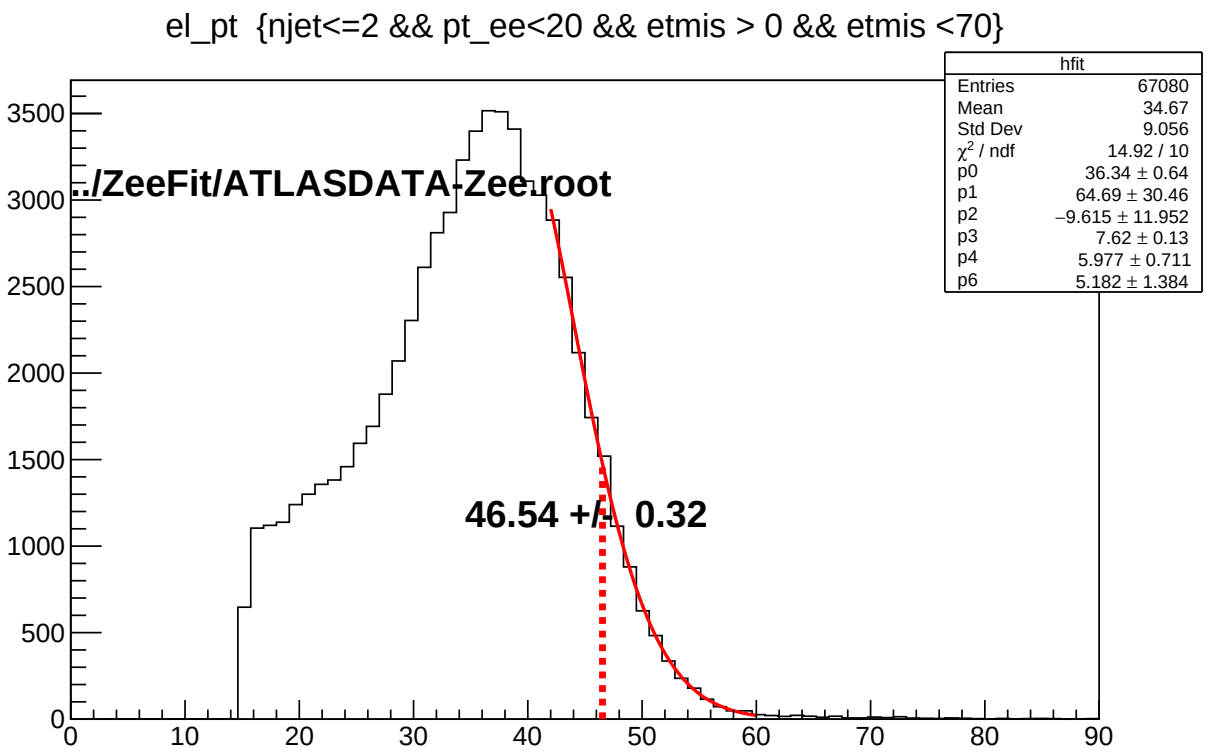

(a) Calibrated data set

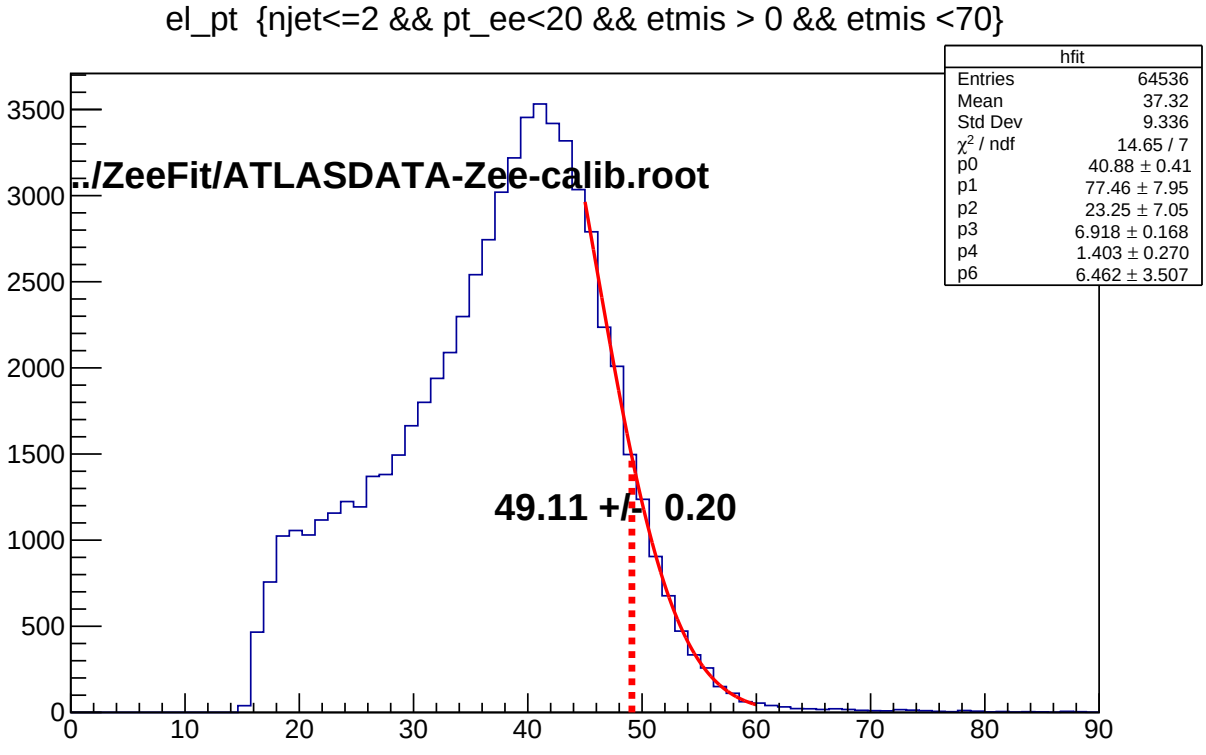

(b) Uncalibrated data set

Figure 17: Half maximum of the ATLAS data set Z $\rightarrow$ *ee* with and without our calibration.

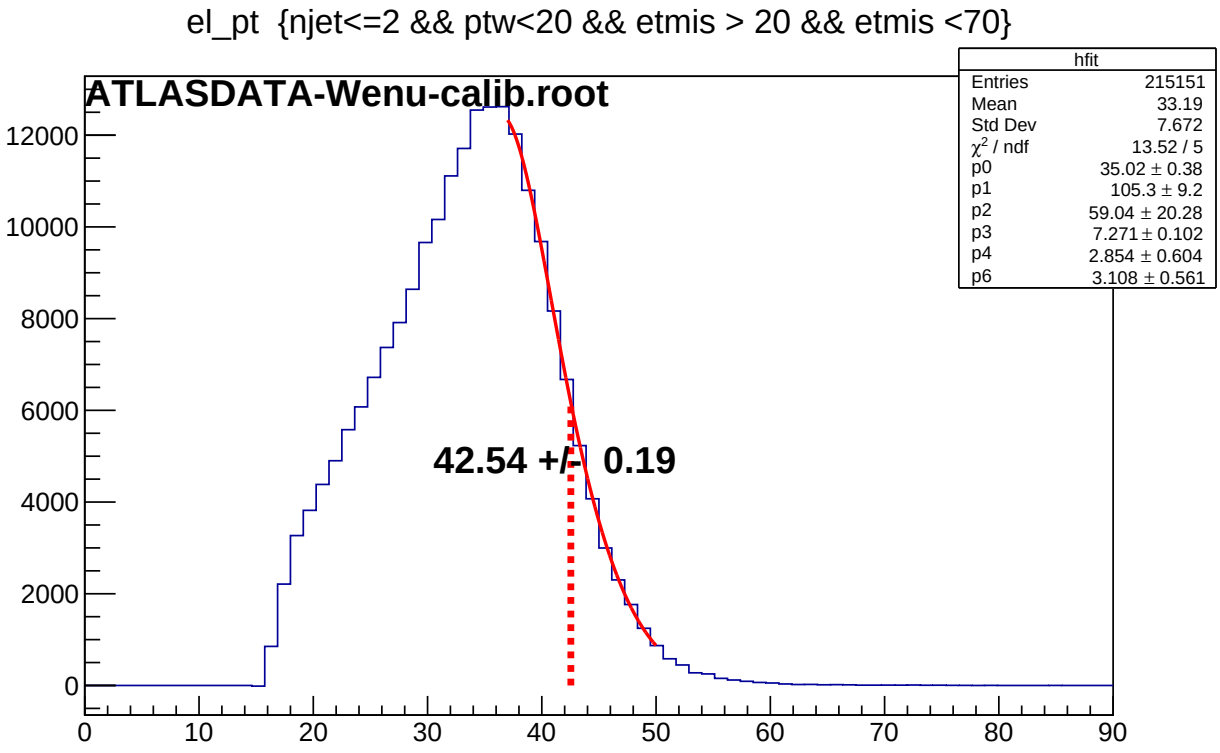

Figure 18: Half maximum of the ATLAS data set for $W \to e\nu$ with subtracting the background.

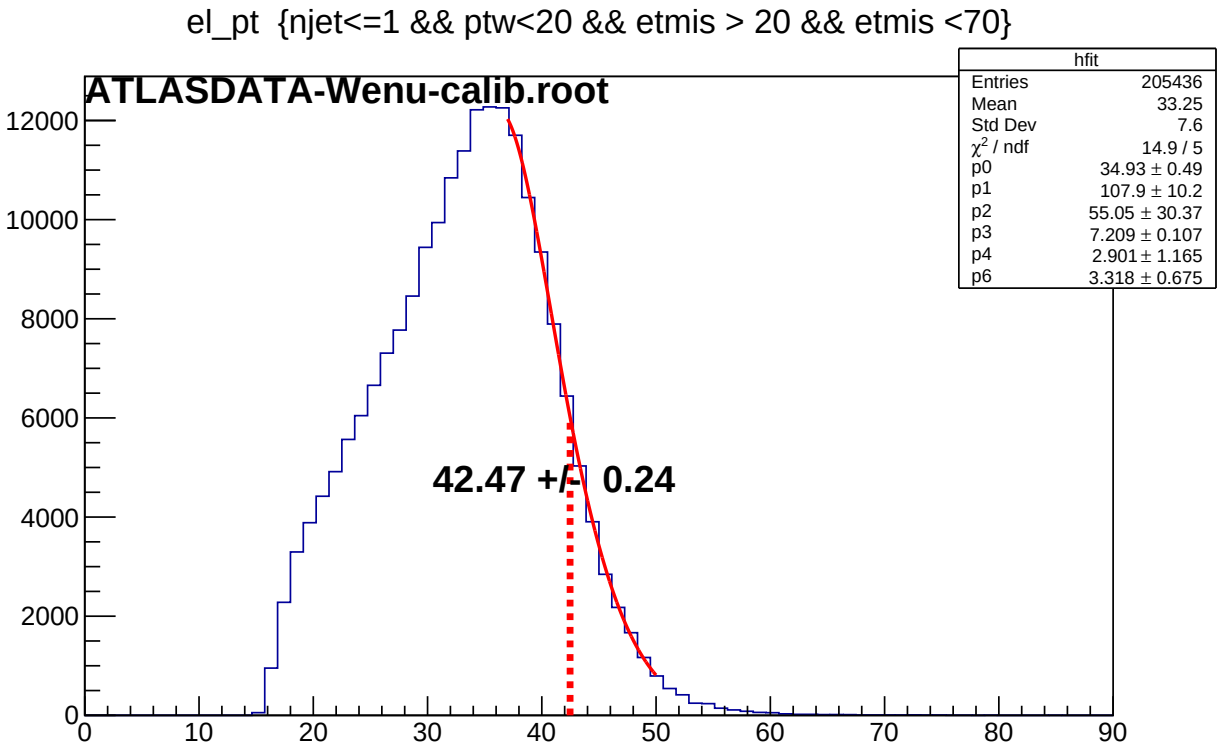

Figure 19: Half maximum of the ATLAS data set for $W \to e\nu$ without subtracting the background.

References

[Bon] Universität Bonn. *Laboratory Course physics601.*

[Ned] Martin zur Nedden. *Physik der schweren Quarks: Von HERA zu LHC.* http://slideplayer.org/slide/495620

[NYU] NYU. *Experimental Particles Physics.* http://physics.nyu.edu/experimentalparticle/history.html.

[Wik] Wikipedia. *Standard Model.* https://en.wikipedia.org/wiki/Standard_Model.

List of Tables

List of Figures